Eur. Phys. J. A **18**, 39–54 (2003)
DOI 10.1140/epja/i2003-10050-2

THE EUROPEAN PHYSICAL JOURNAL A

α-decay spectroscopy of light odd-odd Bi isotopes - I: ^{188,190}Bi nuclei

A.N. Andreyev[1,a], D. Ackermann[2,9], S. Antalic[2,6], H.J. Boardman[1], P. Cagarda[2,6], J. Gerl[2], F.P. Heßberger[2], S. Hofmann[2], M. Huyse[3], D. Karlgren[3,7], A. Keenan[1,4], H. Kettunen[4], A. Kleinböhl[2], B. Kindler[2], I. Kojouharov[2], A. Lavrentiev[5], C.D. O'Leary[1,b], M. Leino[4], B. Lommel[2], M. Matos[2,6], C.J. Moore[1], G. Münzenberg[2,9], R.D. Page[1], S. Reshitko[2], S. Saro[6], H. Schaffner[2], C. Schlegel[2], M.J. Taylor[1,c], K. Van de Vel[3], P. Van Duppen[3], L. Weissman[3,d], and K. Heyde[8,e]

[1] Department of Physics, Oliver Lodge Laboratory, University of Liverpool, Liverpool L69 7ZE, UK
[2] Gesellschaft fur Schwerionenforschung, Planckstrasse 1, D-64291 Darmstadt, Germany
[3] Instituut voor Kern- en Stralingsfysica, University of Leuven, Celestijnenlaan 200 D, B-3001 Leuven, Belgium
[4] Department of Physics, University of Jyväskylä, FIN-40351 Jyväskylä, Finland
[5] Flerov Laboratory of Nuclear Reactions, Joint Institute for Nuclear Research, 141980, Dubna, Russia
[6] Department of Nuclear Physics, Comenius University, SK-84248, Bratislava, Slovakia
[7] Department of Physics, Royal Institute of Technology, 104 05 Stockholm, Sweden
[8] Vakgroep Subatomaire en Stralingsfysica, University of Gent, B-9000 Gent, Belgium
[9] Institut für Physik, Johannes Gutenberg-University, Staudingerweg 7, D-55099 Mainz, Germany

Received: 14 March 2003 / Revised version: 1 May 2003 /
Published online: 2 September 2003 –
Communicated by J. Äystö

Abstract. Detailed fine-structure α-decay studies of ^{188,190}Bi were performed using the complete-fusion reactions of ^{50,52}Cr ions with a ^{142}Nd target at the velocity filter SHIP. The evaporation residues were separated in-flight and subsequently identified on the basis of recoil-α, recoil-α-γ/X-ray and excitation function measurements. Improved data on the α-decay of ^{188,190}Bi were obtained and a number of new low-lying excited states in the daughters ^{184,186}Tl were observed. An intruder, presumably 10^- state was identified in ^{184}Tl, extending the systematics of such states in the odd-odd Tl nuclei beyond the neutron mid-shell at $N = 104$. Some technical aspects of experiment at recoil separators are also discussed.

PACS. 23.60.+e α decay – 27.70.+q $150 \leq A \leq 189$ – 27.80.+w $190 \leq A \leq 219$

1 Introduction

The structure of the neutron-deficient Tl ($Z = 81$) and Bi ($Z = 83$) isotopes has attracted a lot of interest due to a multitude of phenomena occurring in these nuclei. Because of the vicinity to the closed proton shell at $Z = 82$ a systematic appearance of low-lying intruder states is among the most interesting phenomena in this region (see [1–4] and references therein). For example, in the odd-mass Tl nuclei the (normal) $1/2^+$ ground state is produced by the valence $3s^{-1}_{1/2}$ proton π(0p-1h) configuration, while the excitation of a proton across the shell gap at $Z = 82$ to the $1h_{9/2}$ orbital results in a low-lying intruder $9/2^-$, π(1p-2h) state. In the odd-mass Bi nuclei the situation is reversed: the (normal) $9/2^-$ π(1p-0h) ground state coexists with a low-lying $1/2^+$, π(2p-1h) intruder configuration.

The studies of the odd-odd Tl and Bi nuclei are notoriously difficult as the coupling of the odd valence neutron and odd valence proton results in multiplets of states, both normal and intruder, some members of which can become isomeric. In many cases a relatively small energy spacing between the multiplet states and/or the collective bands, built on top of the intruder configurations, further complicate the studies (see [5–7] for examples). As an example of a theoretical study of the p-n multiplets in the odd-odd Tl and Bi nuclei directly relevant to our work we refer to ref. [8].

In this respect α-decay often offers an ideal tool to identify the states in the daughter nucleus which have the

[a] e-mail: aan@ns.ph.liv.ac.uk
[b] *Present address*: Department of Physics, University of York, York, UK.
[c] *Present address*: Department of Physics and Astronomy, Rutgers Univesity, NJ, USA.
[d] *Present address*: NSCL, Michigan State University, East Lansing, MI 48824-1321 USA.
[e] *Present address*: EP-ISOLDE, CERN, CH-1211, Geneva 23, Switzerland.

Table 1. Summary of our results and previous data on the α-decay characteristics of ^{188}Bi. Shown are isomer assignments, α-decay energies E_α, relative intensities I_α, individual half-life values $T_{1/2}$, hindrance factors (HF) and coincident γ-rays. The hindrance factors were calculated with the Rasmussen prescription [9] by assuming $\Delta L = 0$ decays and α-branching ratio of $b_\alpha = 100\%$ for both isomeric states in ^{188}Bi, taken from systematics. The intensities I_α and HF values were normalised to the intensity and HF value of the strongest decay in each isomer, which were assigned values of $I_\alpha = 100\%$ and HF = 1, respectively. The given uncertainties for I_α and HFs include both statistical error and uncertainty of the γ-efficiency determination ($\approx 15\%$) in case of α-γ coincidences

Our data						Reference [10][a]		Reference [11]		Reference [12]		
Isomer, I^π $T_{1/2}$	E_α (keV)	I_α (%)	$T_{1/2}$ (ms)	HF	Coincident γ (keV)	E_α (keV)	I_α (%)	E_α (keV)	$T_{1/2}$ (ms)	E_α (keV)	I_α (%)	$T_{1/2}$ (ms)
^{188m1}Bi, (10^-)	6813(5)	100.0	265(15)	1.0		6820(20)[a]	85(9)	6820(10)[b]	210(87)	6815(6)	100	218(50)
265(15) ms[c]	6995(15)	1.5(5)	160(50)	300(100)	320(1), 249(1)							
	7232(10)	4.5(1.0)	255(20)	600(150)	70.5(5)							
	7302(5)	3.6(1.0)	265(20)	1350(350)								
^{188m2}Bi, (3^+)	6992(5)	100	60(3)	1.0	117.5(5)	7005(25)[a]	15(9)	7010(10)[b]	44(3)	6987(6)	63(5)	46(7)
60(3) ms[d]	6889(10)	0.34(10)	80(20)	132(40)	99.0(5)					6897(18)	9(3)	48^{+28}_{-14}
	(7028(10))[e]							7050	43(29)	7029(7)	28(8)	63^{+50}_{-21}
	7106(5)	2.1(2)	64(5)	120(11)								

([a]) In [10] both 6820(20) and 7005(25) keV α lines were attributed to ^{188}Bi, but no isomer assignment was suggested.
([b]) Quoted in [11] as taken from [10].
([c]) Adopted value from the half-life of the strongest decay at 6813 keV.
([d]) Adopted value from the half-life of the strongest decay at 6992 keV.
([e]) Artificial α line due to α(6992 keV)-e$^-$ summing in the PSSD.

same spin, parity and configuration as in the α-decaying parent. Furthermore, in the region around the $Z = 82$ shell closure the unhindered α-decay is a strong spectroscopic fingerprint for intruder states [7,13]. For example, recent α-decay studies of $^{190-196}$Bi [6,7], along with the complementary in-beam work [5], provided detailed information on the systematic appearance of the normal and intruder excited states in the daughter $^{186-192}$Tl nuclei.

With the aim of extending these investigations to even more neutron-deficient odd-odd Tl and Bi isotopes, we report on a detailed α-decay study of the nucleus ^{188}Bi. Improved data on ^{190}Bi were also obtained in this work. This is a part of our experimental program at the velocity filter SHIP (GSI, Darmstadt) [14–16], with the goal of studying very neutron-deficient Tl-Po nuclei close to and beyond the neutron mid-shell at $N = 104$ [17–19]. The identification of the new isotope ^{184}Bi and improved data on the α-decay of ^{186}Bi are discussed in a companion paper [20].

2 Experimental set-up

The data discussed in this paper resulted from two separate experiments. In the first experiment the fusion reactions ^{142}Nd(^{52}Cr, p3n)^{190}Bi and ^{142}Nd(^{52}Cr, p5n)^{188}Bi were used, while in the second experiment ^{188}Bi was produced in the ^{142}Nd(^{50}Cr, p3n)^{188}Bi reaction. The rotating target, made of isotopically enriched $^{142}NdF_3$ material (99.8% enrichment, 290 μg/cm^2 thickness), the experimental set-up and detection system were similar in both experiments and their detailed description was given in [15,17]. Enriched ^{50}Cr or natural ^{52}Cr materials were used and pulsed beams (5 ms on/15 ms off) of up to 500 pnA were provided by the UNILAC heavy-ion accelerator. In both experiments the data were collected at a few beam energies varied in a step of about 5 MeV within the range of 380–480 MeV to allow for excitation function measurements.

The evaporation residues (EVRs) after separation were implanted into a 300 μm thick, 35 × 80 mm^2 16-strip position-sensitive silicon detector (PSSD), where their subsequent α-decays were measured. The energy resolution of each strip was typically about 18 keV at α-decay energies of 7–8 MeV. Behind the PSSD a fourfold segmented Clover detector was installed for prompt and delayed (0–5 μs) α-γ/X-ray coincidence measurements. Timing measurements with the time-to-amplitude converter (TAC) could not be used in the first experiment (with ^{52}Cr, [17]). The TAC was used in the second experiment (with ^{50}Cr), which allowed us to collect much cleaner α-γ coincident spectra. The absolute efficiency measurements of the Clover detector were discussed in detail in [17]. Singles data (EVRs or α-decay) and coincidence data (α-γ/X-rays) were collected during the experiment.

3 Experimental results

3.1 α-decay of ^{188}Bi

The previous studies [10–12] identified two α-decaying isomeric states in ^{188}Bi (see table 1). In our experiments we were able to produce this isotope with at least two orders of magnitude higher statistics than in [11,12]. No experimental spectra or production yields of ^{188}Bi were given in [10], in which this isotope was identified for the first time.

Figure 1a,b show the α spectra measured at beam energies of $E(^{50}\text{Cr}) = 238$ MeV and 252 MeV in front of the target, which correspond to the maxima of the excitation functions of ^{189}Bi and ^{188}Bi, respectively. The observation of α lines at 6813(5) keV, 6992(5) keV and 7028(10) keV in fig. 1b confirms the previously published

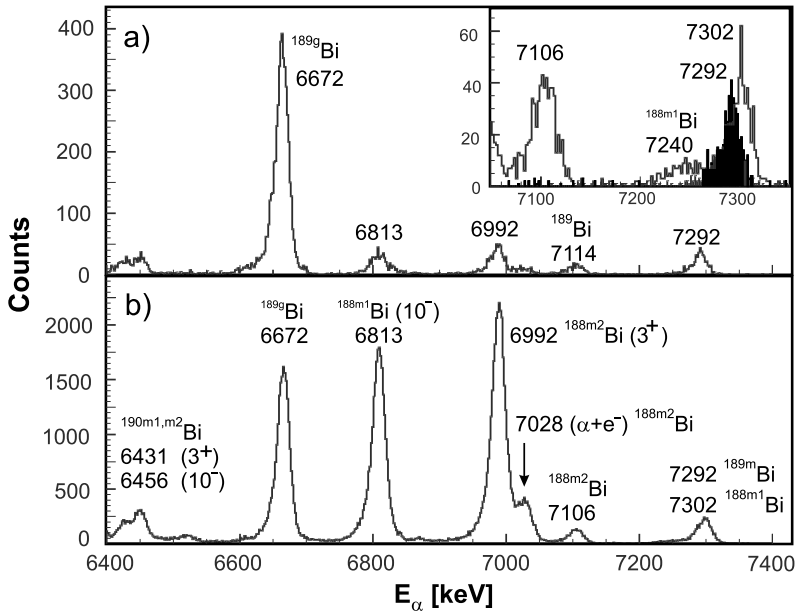

Fig. 1. Energy spectra of the α-decays in the PSSD, collected between the beam pulses at beam energies of $E(^{50}\mathrm{Cr}) =$ 238 MeV (a) and 252 MeV (b). The inset shows the overlay of the spectra, produced in the recoil-α correlation analysis of the events from fig. 1b, with the time constraint of ΔT(recoil-α) = (0–5) ms (full histogram) and (50–600) ms (open histogram). Some peaks are labelled with the α-decay energy (in keV) and the isotope to which the α-decay belongs.

data for ^{188}Bi (see table 1), although, as discussed below, a new interpretation will be given to the last α line. A slight difference in the α-decay energies, deduced in different experiments (table 1), is most probably related to the use of different α lines for calibration. In this work the known abundantly produced α-decays of ^{186}Pb (5980(5) keV [21]) and of ^{189}Bi have been used. The nucleus ^{189}Bi has two α-decaying isomeric states with the strongest α lines (see fig. 1a) at 6672 keV (^{189g}Bi, $T_{1/2}$ = 728(40) ms) and 7292 keV (^{189m}Bi, $T_{1/2} = 5.0(1)$ ms), respectively, see [17, 12] and references therein. As will be shown below, some α-decays of ^{188,189}Bi have similar decay energies and they could be distinguished from the excitation function measurements and/or half-life differences.

From the time distributions between the recoil implantation and subsequent α-decays (recoil-α time-position correlation analysis [15,16]) more precise half-life values of 265(15) ms and 60(3) ms were deduced for the 6813 keV and 6992 keV α lines of ^{188}Bi, respectively. In the following discussion the longer-lived and the shorter-lived isomers of ^{188}Bi will be denoted by ^{188m1}Bi and ^{188m2}Bi, respectively, with the corresponding daughter isomers denoted as ^{184m1}Tl and ^{184m2}Tl.

The time distribution of the events in the peak, denoted as 7292–7302 keV in fig. 1b clearly shows two distinct components with half-life values of 4.9(5) ms and 265(20) ms (see fig. 2a). This fact suggests that at least two different activities with quite similar decay energies contribute to the peak. This is further confirmed by the inset to fig. 1, which shows an overlay of two α spectra obtained from the correlation analysis of the events from fig. 1b with a time constraint of ΔT(recoil-α) = 0–5 ms (filled histogram) and 50–600 ms (open histogram). Four

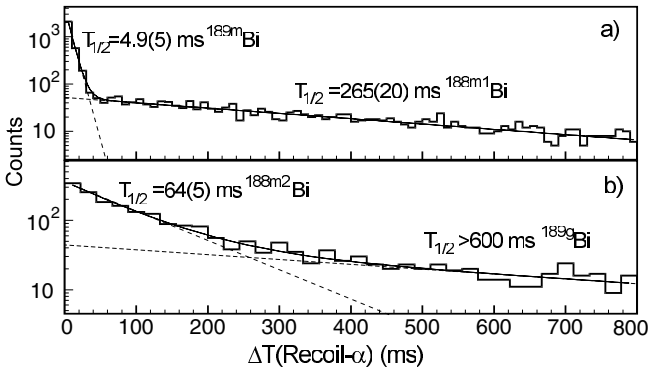

Fig. 2. Time distributions of the events in the peak at 7292–7302 keV of fig. 1b (a) and of the events in the peak at 7106 keV (b). The continuous solid lines show the result of a simultaneous fit by two exponential curves, shown separately by dashed lines. The deduced half-life values and isotope assignments for the different components are given.

peaks at 7106, 7240, 7292 and 7302 keV are seen in the inset. The peak at 7292 keV ($T_{1/2}$ = 4.9(5) ms), shown by the filled histogram, was assigned to the known decay of ^{189m}Bi. The number of the 7292 keV decays in the peak at 7292–7302 keV of fig. 1b can be easily estimated either from the time distribution spectrum, shown in fig. 2a, or by using the following simple consideration. As seen from fig. 1a, the α-decay of ^{189}Bi is the strongest one at the beam energy of 238 MeV, at which the contribution from ^{188}Bi is about an order of magnitude lower. The intensity ratio of the 6672 keV and 7292 keV peaks of ^{189}Bi at this beam energy is $I_\alpha(6672)/I_\alpha(7292) = 10.0(5)$ (fig. 1a), while the corresponding ratio at the beam energy

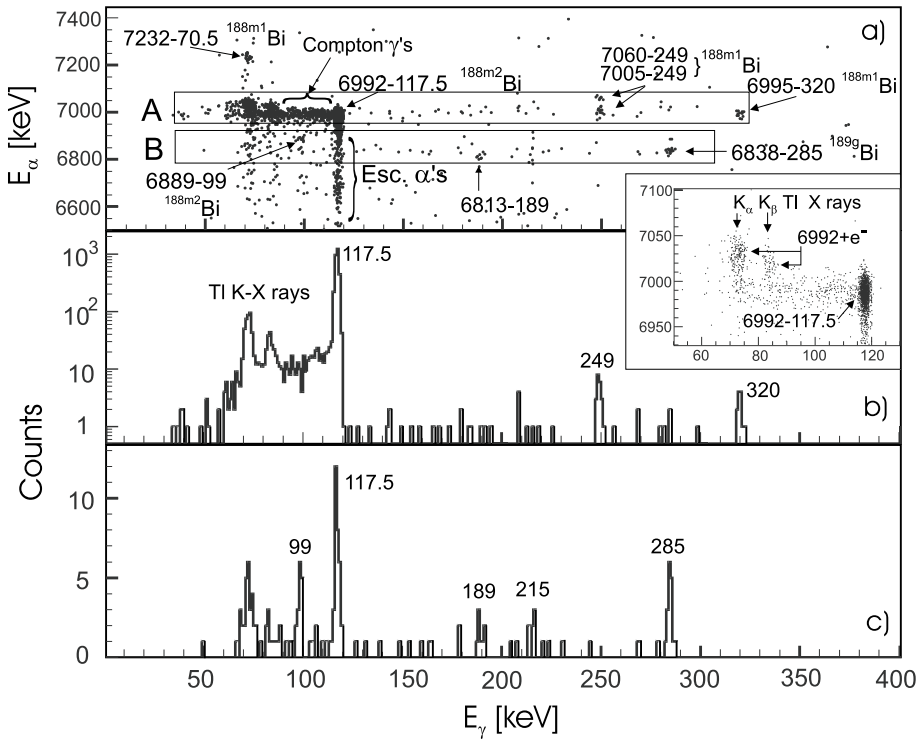

Fig. 3. a) Prompt α-γ matrix, observed at the beam energy of $E(^{50}\mathrm{Cr}) = 252$ MeV; panels b) and c) show projections on the γ energy axis of the events from the rectangles A and B of a), respectively. The inset shows an expanded part of a) for the 6992 keV α line, which illustrates the effect of the α-e$^-$ summing, discussed in the text. Some groups of α-γ coincident events are denoted with the corresponding α and γ energies.

of 252 MeV is $I_\alpha(6672)/I_\alpha(7292\text{–}7302) = 6.1(2)$ (fig. 1b). Clearly, the lower ratio value in the latter case should be attributed to the contribution of the peak at 7302(5) keV.

In such a way the contribution of the 7292 keV decay of ^{189}Bi in the α peak around 7300 keV at each beam energy was reliably estimated and the excitation functions for the 7292 keV and 7302 keV peaks were obtained. The excitation function of the 7302 keV peak was found to be similar in shape and position to those for the strongest α-decays of ^{188}Bi. Therefore, based on the deduced half-life value of 265(20) ms, we assign the peak at 7302(5) keV to the α-decay of the longer-lived isomer $^{188\mathrm{m1}}$Bi. That is why the 6813 keV decay of $^{188\mathrm{m1}}$Bi establishes a new excited state at 500(5) keV above the state in the daughter $^{184\mathrm{m1}}$Tl, which is fed by the 7302(5) keV decay.

Figure 3 shows a prompt α-γ coincidence matrix and two projections on the γ energy axis, collected at the beam energy of 252 MeV. The inset shows an expanded part of fig. 3a for the specific case of the 6992 keV decay of $^{188\mathrm{m2}}$Bi. We stress that the requirement of prompt coincidences limits the multipolarity of all the transitions in fig. 3 to $E1$, $M1$ and $E2$.

The strongest group of α-γ coincident events at 6992(5) keV–117.5(5) keV in fig. 3a (measured half-life $T_{1/2} = 59(3)$ ms) confirms the results of the unpublished work [11], in which the 7010(10) keV–117 keV events were found. We also note two groups of events, denoted as "Compton γ's" and "Esc. α's", which are usually observed in the α-γ spectra in such experiments. The former group results when a Compton scattered γ-ray (small-angle scattering of the 117.5 keV transition in the aluminium vacuum chamber, in the detector cryostat window and/or in the Ge crystal itself), is registered in the Clover detector in coincidence with a full energy 6992 keV α-decay, observed in the PSSD. The latter group results when a full energy 117.5 keV γ-ray is registered in coincidence with an α-particle of 6992 keV, escaping from the PSSD in the backward direction and leaving only a part of its energy in the PSSD.

In ref. [11], based on the assumed upper limit of $\alpha_K < 0.1$ for the K-conversion coefficient (no K X-rays have in fact been observed), a tentative suggestion of an $E1$ multipolarity was made for the 117 keV transition (as the theoretical conversion coefficients are $\alpha_K(E1) = 0.23$, $\alpha_K(E2) = 0.5$, $\alpha_K(M1) = 5$ [22]). Due to the much higher number of events in our experiment, the 6992 keV decay has also been observed in coincidences with the K X-rays of the Tl daughter nuclei (see fig. 3a,b and inset). Therefore, by comparing the number of the full energy $E_\gamma = 117.5$ keV events with the number of the K X-rays in fig. 3b the conversion coefficient of $\alpha_K(117.5\text{ keV}) = 0.27(5)$ was deduced, which unambiguously establishes an $E1$ multipolarity for this transition.

An important, but often overlooked effect of the α-conversion electron energy summing in the silicon detector in experiments with implanted activity is worthy of mention with respect to fig. 3a,b. Namely, due to the recoil implantation at a typical depth of a few micrometers

in the PSSD, the energy of fine-structure α-decay, feeding an excited state, which decays by an (at least, partially) converted transition, will sum with the energy of the subsequent conversion electron (plus the energy of the Auger electrons, see below). Clearly, the total energy, registered in the PSSD, depends both on the direction and on the energy of the conversion electrons. A few examples of this effect will be discussed below.

As an example, the inset to fig. 3 illustrates the energy summing of the 6992 keV decay of ^{188m2}Bi with the conversion electrons of $E_{e^-} = 117.5$ keV $- B_{e^-}(K) \approx 32$ keV ($B_{e^-}(K) = 85.5$ keV is the electron binding energy in the K-shell of the daughter Tl nuclei). In this particular case, due to a rather low conversion electron energy it will practically fully sum in the PSSD with the energy of the coincident α-decay, resulting in an artificial peak with a total energy of $\approx$ 7030 keV, which is in coincidence with K X-rays. Exactly such a pattern is seen in the inset of fig. 3, which shows two groups (denoted as $6992 + e^-$) at $\approx$ 7032(10) keV and $\approx$ 7024(10) keV in coincidences with the K_α and K_β X-rays of Tl. The difference of about 10 keV between these energies arises due to additional summing with the Auger electrons in case of K_α-conversion. On these grounds, we interpret the α line at 7028(10) keV in fig. 1b and fig. 3, along with the lines at 7050 keV, 7029(7) keV of refs. [10,12], as artificial ones, resulted from such α-e^- summing. These conclusions are also confirmed by our Monte Carlo simulations, based on the GEANT program [23]. Such summing effects have been also discussed in [17,24] and we refer the reader to these papers for more details.

The 6992 keV-117.5 keV α-γ coincidences suggest a possibility for a full energy (crossover) α-decay with $E_\alpha =$ 7107 keV in ^{188m2}Bi. Indeed an α line at $E_\alpha = 7106(5)$ keV was observed in fig. 1b. However, the isotope ^{189}Bi has two α-decays with a quite similar energy of 7114 keV (see fig. 1a and [12]). Applying the method discussed above for the separation of the 7292 keV–7302 keV α lines, we compare the intensity ratio I_α(6672 keV)/I_α(7106–7114 keV) of 21.8(2) and 9.3(2), deduced from figs. 1a and 1b, respectively. This comparison shows that the α peak at 7106 keV in fig. 1b has more counts than one would expect from ^{189}Bi only. By using the 6672 keV peak as a measure of ^{189}Bi and applying the ratio of 21.8, we estimated the contribution of ^{189}Bi to the 7106 keV peak at the different beam energies used. In this way the excitation function for the decay at 7106–7114 keV can be decomposed into two components with the maxima separated by about 15 MeV. The one at the lower beam energy is clearly due to ^{189}Bi, while the shape and position of the second component fit to those of the 6992 keV and 6813 keV decays of ^{188}Bi. Moreover, the time distribution of the 7106 keV α line, deduced from the recoil-α analysis at the beam energy of 252 MeV, clearly shows a component with a half-life of $T_{1/2} = 64(5)$ ms (see fig. 2b), matching the half-life of the 6992 keV α-decay. On these grounds we assign the α-decay at 7106 keV with the half-life of 64(5) ms to the crossover decay of the short-lived isomer ^{188m2}Bi.

A group of prompt coincident events at 7232(10) keV-70.5(5) keV in fig. 3a has a half-life of $T_{1/2} = 255(20)$ ms and $Q_{\alpha,\mathrm{sum}} = Q_\alpha + E_\gamma = 7460(10)$ keV, which are consistent with the corresponding values of ^{188m1}Bi ($Q_\alpha =$ 7461(5) keV for the 7302 keV decay). Therefore, the 7232(10) keV group was assigned to a fine-structure decay of ^{188m1}Bi to a new excited state at 70.5(5) keV in the daughter nucleus ^{184}Tl. This transition should be converted, either rather weakly in the case of an $E1$ multipolarity ($\alpha_{\mathrm{tot}}(E1, \mathrm{theor.}) = 0.21$), or strongly in the case of an $M1$ ($\alpha_{\mathrm{tot}}(M1, \mathrm{theor.}) = 4.2$) or $E2$ ($\alpha_{\mathrm{tot}}(E2, \mathrm{theor.}) = 110$) multipolarity [22]. As in the case of the 6992 keV-117.5 keV α-γ coincidences, the energy of the low-energy electron ($E_{e^-} \approx 57$ keV), resulting from the L-conversion of the 70.5 keV transition, will be fully or partially summed in the PSSD with the energy of the feeding 7232 keV decay. According to GEANT calculations, this effect produces a double-humped structure with a lower-energy peak around 7240 keV and a higher-energy peak around 7290 keV. The former peak, seen in the inset to fig. 1, results when the electron escapes from the PSSD in the backward direction, thus leaving only part of its energy ($\approx$ 10 keV, [17]) in the PSSD. The latter peak (masked by the more abundant tail of the 7302 keV decay of ^{188m1}Bi) arises when the electron is fully registered in the PSSD. The intensity ratio between the two peaks $I_\alpha(7240)/I_\alpha(7290) = 1 : 2.0(3)$ was deduced from the GEANT simulations. Therefore, the *total* number $N_\alpha(7232)$ of the 7232 keV decays can be deduced from the number of the 7240 keV counts in the inset to fig. 1, corrected for the above ratio. By comparing this number and the number $N_{\alpha\gamma}$ of the 7232 keV-70.5 keV coincident events (after normalisation for the γ-efficiency at 70.5 keV) the total conversion coefficient of the 70.5 keV transition was deduced as $\alpha_{\mathrm{tot}} = (N_\alpha(7232)\text{-}N_{\alpha\gamma})/N_{\alpha\gamma} =$ 5(1), which unambiguously establishes an $M1$ multipolarity for this transition.

Three groups of the prompt α-γ coincident events at 6995(15) keV-320(1) keV, 7005(15) keV-249(1) keV and 7060(15) keV-249(1) keV in fig. 3a have similar half-life values of 160(50) ms. Furthermore, the 6995-320 keV group has the value of $Q_{\alpha,\mathrm{sum}} = 7467(15)$ keV which is compatible with the value of $Q_\alpha = 7461(5)$ keV for the 7302 keV decay of ^{188m1}Bi. On these grounds the 6995(15) keV α-decay was assigned to a fine-structure decay of ^{188m1}Bi to a new excited state at 320(1) keV in the daughter nucleus ^{184}Tl, see fig. 4. The somewhat shorter half-life is still in agreement within the statistical uncertainty with the value of $T_{1/2} = 265(15)$ ms for the strongest 6813 keV decay of ^{188m1}Bi. On the other hand, as will be shown in the discussion, we cannot rule out a possibility that the 320 keV state is also partly fed by the 6992 keV decay of the shorter-lived ^{188m2}Bi, which would explain the measured shorter half-life value of the 6995-320 keV coincident events.

The energy of the peak at 249(1) keV in fig. 3b is practically equal to the energy difference between the 320 keV and 70.5 keV states in ^{184}Tl, which suggests that the excited state at 320 keV decays also via a cascade of 249 keV

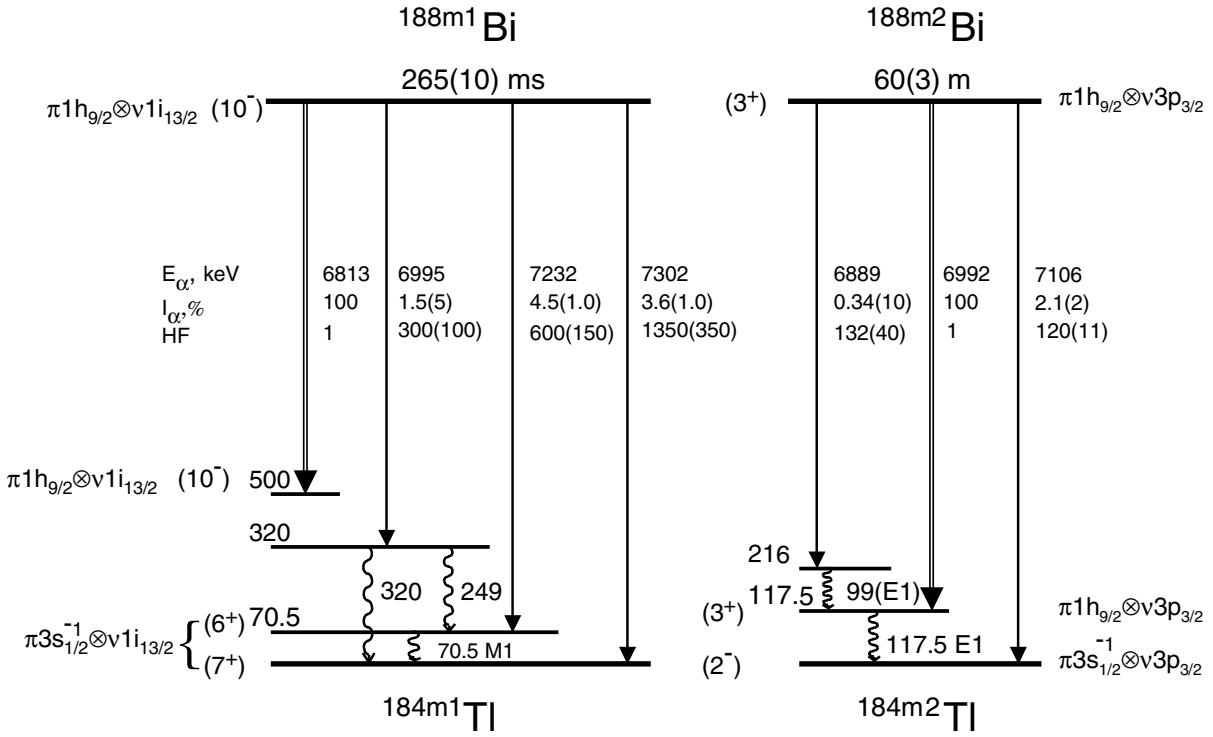

Fig. 4. The α-decay scheme of ^{188m1,m2}Bi deduced from this work. Spin and parity assignments are tentative. The strongest (unhindered) α-decays are shown by a thick line. The relative positions of the isomers in ^{188}Bi and in ^{184}Tl are not known.

and 70.5 keV transitions. This, together with a rather large conversion coefficient of the 70.5 keV transition provides a natural explanation for the presence in fig. 3a of two groups of events at 7005(15) keV and 7060(15) keV (rather than a single group at 6995(15) keV) in coincidence with the 249 keV transition. The energy shift in both cases results from the partial (if the electron escapes from the PSSD) and full α(6995 keV)-e$^-$ energy summing, respectively, with the electrons from the L-conversion of the 70.5 keV decay (cf. the discussion of the 7240 keV and 7290 keV peaks resulting from the α(7232 keV)-e$^-$ summing).

A group of prompt α-γ coincident events at 6889(10) keV-99.0(5) keV (see fig. 3a,c) has the values of $Q_{\alpha,\mathrm{sum}} = 7138(10)$ keV and $T_{1/2} = 80(20)$ ms, which are consistent with the values of $Q_\alpha = 7144(5)$ keV and $T_{1/2} = 60(3)$ ms, respectively, for the strongest 6992 keV decay of ^{188m2}Bi. On this basis we assign the 6889(10) keV decay as originating from the latter isomer and feeding an excited state at 99 keV above the state at 117.5 keV, thus at 216(1) keV, in ^{184}Tl. In this case the triple 6889 keV-99 keV-117.5 keV coincidences should be observed as well. However, in the region of 6889 keV-117.5 keV in fig. 3a there are events resulting from the coincidences between the escaping α-particles from the 6992 keV decay and the full energy γ-rays at 117.5 keV (marked as "Esc. α's"). This prohibits us from drawing a reliable conclusion about the presence of such triple coincidences.

Based on the upper limit of 3 counts for the number of the K X-rays in coincidence with the 6889 keV decay (fig. 3a), an upper limit of $\alpha_K \leq 0.20(14)$ for the K-conversion coefficient of the 99 keV decay can be deduced. This tentatively establishes an $E1$ multipolarity for this transition as $\alpha_K(E1, \mathrm{theor.}) = 0.36$, $\alpha_K(M1, \mathrm{theor.}) = 7.5$, $\alpha_K(E2, \mathrm{theor.}) = 0.58$.

We mention that in [12] a weak decay with a few counts only was observed at 6897(18) keV and attributed to the short-lived isomer in ^{188}Bi (see table 1). This decay and the decay at 6889(10) keV, discussed above, could represent the same decay, although the intensity deduced in [12] for the 6897(18) keV decay was much higher.

Finally, we note a group of 8 α-γ events at 6813(10) keV-189(1) keV in fig. 3a,c. The α-decay energy and the half-life $T_{1/2} = 250(20)$ ms of this group are consistent with the values for the strongest decay of ^{188m1}Bi. This decay would suggest the presence of the 189 keV transition in ^{184m1}Tl, but the absence of any further coincidences does not allow us to draw any conclusion on the nature of this decay.

The decay scheme of ^{188}Bi, based on the previous data and our work, is shown in fig. 4 and will be discussed in sect. 4.

3.2 α-decay of ^{190}Bi

Previous studies identified two long-lived isomeric states in ^{190}Bi with nearly the same half-lives and tentative I^π assignments of (10^-) and (3^+), see table 2. In the following discussion the high- and the low-spin isomers of ^{190}Bi

Table 2. Summary of our results and previous data on the α-decay characteristics of ^{190}Bi. The hindrance factors were calculated with the Rasmussen approach [9] by assuming $\Delta L = 0$ decays and using the half-life values and branching ratios taken from [7] and shown in the first column of the table. The intensities I_α and HF values, including those from [7], were normalised to the intensity and HF value of the strongest decay in each isomer, which were assigned values of $I_\alpha = 100\%$ and HF = 1, respectively. The given uncertainties for I_α and HFs include both statistical error and uncertainty of $\approx 15\%$ of the γ-efficiency determination in case of α-γ coincidences.

Our data					Reference [7]			
Isomer, I^π $T_{1/2}$, b_α	E_α (keV)	I_α (%)	HF	Coincident γ (keV)	E_α (keV)	I_α (%)	HF	Coincident γ
^{190m1}Bi, (10^-)	6392(10)	0.24(4)	235(40)	352,441				
5.9(6) s, 70(9)%	6456(5)	100	1	373.9[a]	6456(5)	100	1[b]	373.9[a]
	6472(10)	0.41(7)	275(50)	(75), 281, 267, 356				
	6546(10)	0.046(8)	4700(800)	281				
	6570(10)	0.039(8)	6600(1200)	255				
	6734(10)	1.5(2)	750(120)	89	6734(5)	1.5(2)	750(200)	89.5
	6819(10)	2.0(3)	1100(200)		6819(5)	1.7(2)	1300(300)	
^{190m2}Bi, (3^+)	6225(10)	0.06(1)	240(4)	213				
5.7(8) s, 90^{+10}_{-30}%	6412(10)	0.10(2)	700(150)	314				
	6431(5)	100	1	294	6431(5)	100	1[b]	78.5, 293.7
	6507[c]				6507(5)	0.24(8)	816(40)	
	6611(10)	2.2(3)	230(40)	105				
	6716(10)	1.5(2)	700(100)		6716(5)	2.0(3)	575(20)	

[a] Delayed transition, not actually seen in the α-γ coincidences as it de-excites the 2.9 s 374 keV excited state in ^{186m1}Tl (data taken from [7]).
[b] Actual HF values, deduced in [7], are: HF = 2.0(4) for ^{190m1}Bi (10^-) and HF = $1.2^{+0.5}_{-0.3}$ for ^{190m2}Bi (3^+).
[c] Not observed in our data, but assumed from the data of [7], see text.

decaying by 6456(5) and 6431(5) keV α emission, respectively, will be denoted as ^{190m1}Bi and ^{190m2}Bi, while the corresponding daughter isomers are ^{186m1}Tl and ^{186m2}Tl.

Despite a relatively low cross-section of the ^{142}Nd(^{50}Cr, pn)^{190}Bi reaction, the α-decays of 6431(5) and 6456(5) keV were also observed in the second experiment (see fig. 1a,b). However, the main data discussed in this work were collected in the first experiment in the ^{142}Nd(^{52}Cr, p3n)^{190}Bi reaction at a beam energy of 256 MeV in front of the target. In total about 10^6 α-decays of each isomeric state in ^{190}Bi were observed, see fig. 1 of [18], which gives an example of the collected spectra. We confirmed the data of ref. [7], and, due to the two orders of magnitude higher number of decays collected in our experiment, a more detailed study was possible. Unfortunately, because of a rather high implantation rate in the PSSD, no half-life information could be deduced for the relatively long-lived isomers in ^{190}Bi. Therefore, the assignment of the fine-structure α-decays was done on the basis of a Q_α value analysis and on α-γ-γ coincidence relations, if possible.

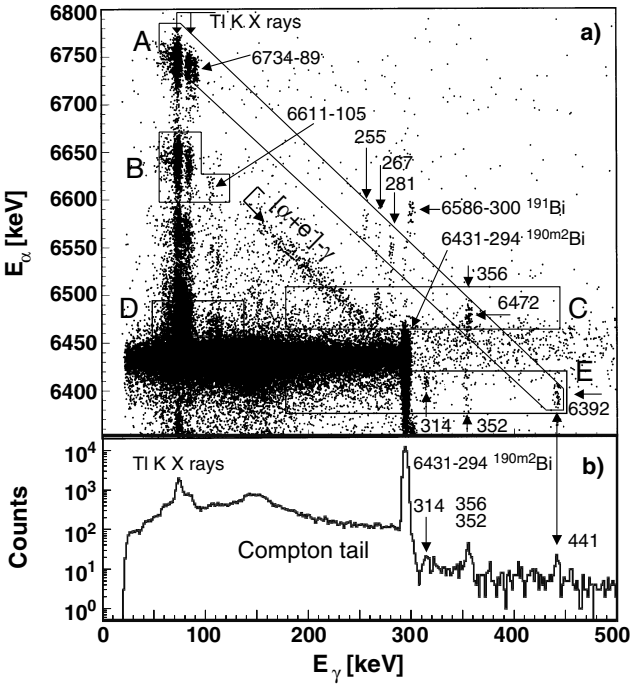

Fig. 5. a) The α-γ matrix, observed at the beam energy of $E(^{52}\mathrm{Cr}) = 256$ MeV; b) projection on the γ energy axis of all events from a). The projections from the boxes denoted by A-E are shown in fig. 6.

3.2.1 The α-decay of the high-spin isomer

Figure 5a shows part of the α-γ matrix, collected in this experiment. As no TAC was used, all α-γ coincidences were measured within a fixed time interval of $\Delta T(\alpha\text{-}\gamma) =$ (0–5) μs. Although this resulted in a larger random background in the α-γ matrix compared to the second experiment, a reliable identification was possible in practically all the cases as shown below.

Figure 5b shows a projection on the γ energy axis of all events from fig. 5a. The dominant 6431(5) keV-294.0(5) keV coincident group in fig. 5a,b with about 5×10^4 counts is the known strongest fine-structure decay

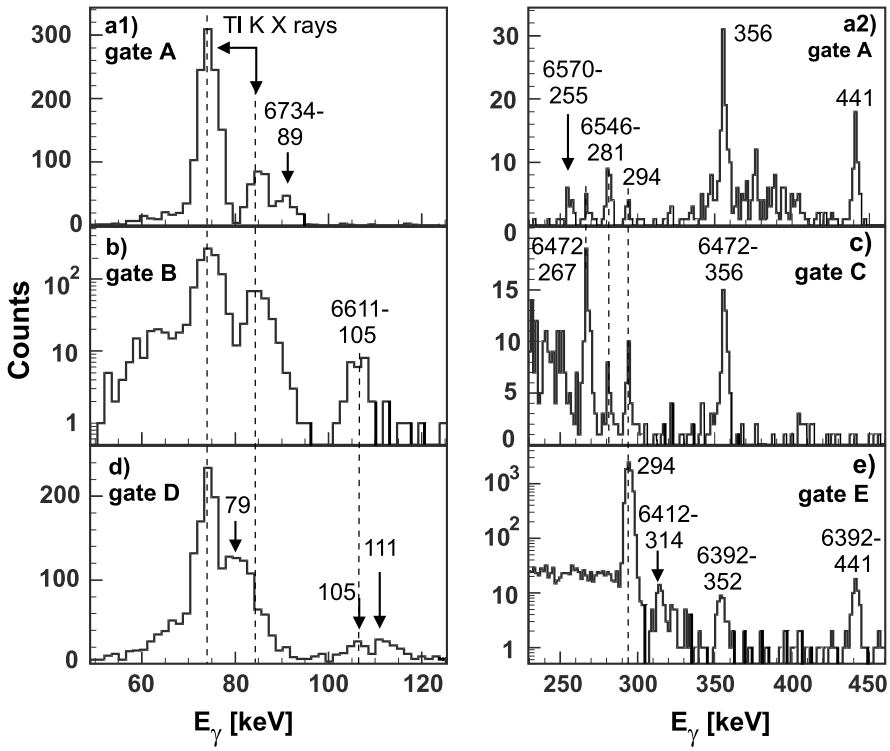

Fig. 6. Projections on the γ energy axis of events from frames A-E of fig. 5a. Some γ peaks are labelled with the corresponding α and γ energies of the α-γ coincident pairs. Note the logarithmic scale in parts b) and e).

of the low-spin isomer in ^{190}Bi [7]. As in fig. 3a, the Compton-scattered γ events and escaping α-particles are clearly seen in fig. 5.

An interesting effect which produces the events along the diagonal line denoted by "$[\alpha + e^-]$-γ" in fig. 5a and which becomes visible only in experiments with a high statistics is worthy of mention. In our case the events result from a prompt multistep process which involves the forward-angle Compton scattering of the 294 keV γ-rays in the relatively *thin* PSSD. The resulting Compton electrons are registered in the PSSD and sum up with the energy of the feeding 6431 keV α-decay. The prompt coincidences of such $\alpha + e^-$ events with the Compton scattered γ-rays escaping from the PSSD and being registered in the Clover detector, produce the observed events along the sloped line. The GEANT simulations [23] confirm this effect, which produces an additional background along the line of possible fine-structure α-decays of ^{190m2}Bi with a constant value of $Q_{\alpha,\mathrm{sum}} = 6863(5)$ keV. This value corresponds to the $Q_{\alpha,\mathrm{sum}}$ value of the strongest 6431 keV-294 keV coincident events of ^{190m2}Bi.

A few weaker (by $\approx 10^3$ times) groups of coincident events can be seen in fig. 5a,b and in the γ spectra, which were registered in coincidence with new α-decays of ^{190}Bi (see fig. 6).

Frame A in fig. 5a defines the region of possible fine-structure α-decays of the high-spin isomer ^{190m1}Bi with a constant value of $Q_{\alpha,\mathrm{sum}} = 6969(5)$ keV, which corresponds to the $Q_{\alpha,\mathrm{sum}}$ value of the strongest 6456 keV-374 keV decay. The α-γ groups at 6392(10)-441(1), 6472(10)-356(1), 6546(10)-281(1) , 6570(10)-255(1) and 6734(10)-89(1) keV, all having the same value of $Q_{\alpha,\mathrm{sum}} = 6967(10)$ keV, were observed in this frame. For further discussion, fig. 6a1,a2 show the low- and the high-energy parts of the projection on the γ energy axis of the events inside frame A of fig. 5a.

In the low-energy part (fig. 6a1) along with the Tl K X-rays, a peak at 89(1) keV is seen in coincidence with the 6734 keV α-decay. It confirms the identification of this decay made in [7] (at $E_\gamma = 89.5(4)$ keV). By comparing the numbers of the Tl K X-rays and 89 keV decays, a more precise K-conversion coefficient of $\alpha_K = 10.3(9)$ (compared to $\alpha_K = 17(8)$ from [7]) was deduced, which unambiguously establishes a pure $M1$ multipolarity for this decay ($\alpha_K(M1, \mathrm{theor.}) = 10.2$).

Based on the $Q_{\alpha,\mathrm{sum}}$ value analysis, the above-mentioned groups of events were assigned as the fine-structure α-decays of ^{190m1}Bi feeding the new excited states at 255, 281, 356 and 441 keV in the daughter nucleus ^{186m1}Tl (see table 2 and fig. 7).

Apart from the 6392 keV-441 keV coincidences, the α-decay at 6392 keV is also seen in coincidence with the 352 keV transition (fig. 6e), which shows the events from box E of fig. 5a. The latter decay presumably feeds the state at 89(1) keV in ^{186}Tl, as the energy difference of 441 keV − 352 keV = 89 keV fits to this energy. The presence of the 294 keV γ-decay in fig. 6e is due to escaping α-particles of the 6431 keV decay which are also found within box E. The peak at 314 keV is attributed to ^{190m2}Bi (see below).

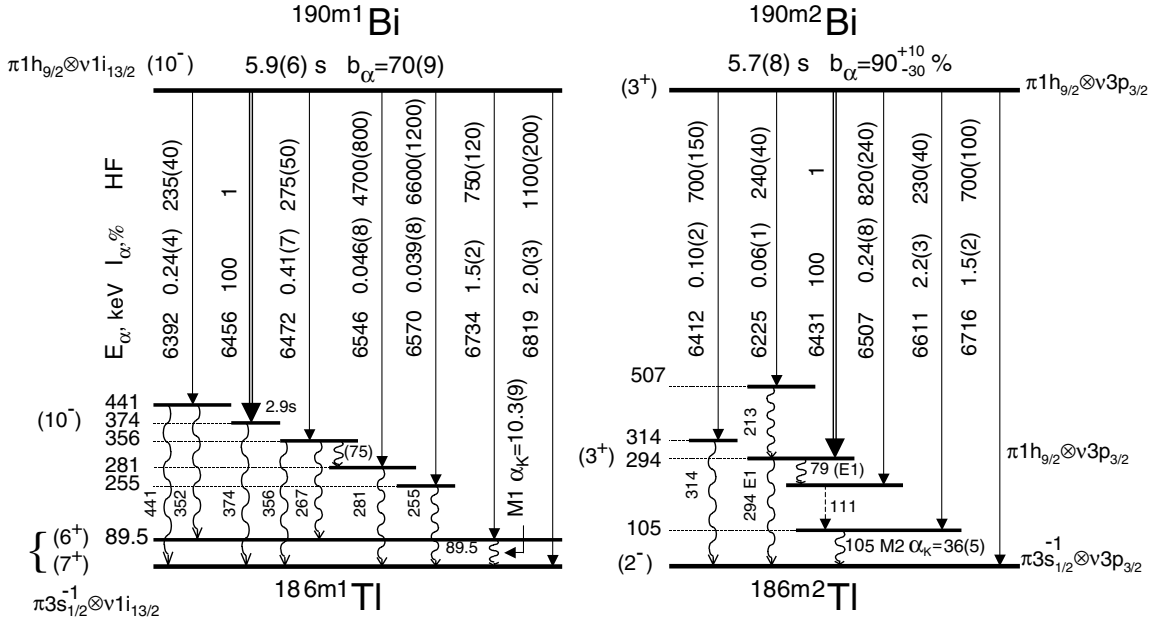

Fig. 7. The α-decay scheme of ^{190m1,m2}Bi. All the spin and parities are tentative. The strongest (unhindered) α-decays are shown by a thick line. The half-life and branching ratio b_α values were taken from [7]. The relative positions of the isomers in ^{190}Bi and in ^{186}Tl are not known.

Similarly, in addition to the 6472 keV-356 keV coincidences, the α-decay at 6472 keV was observed in coincidences with the 267 keV and 281 keV γ-decays, see fig. 6c. The energy difference of 356 keV − 267 keV = 89 keV suggests that the 267 keV transition feeds the excited state at 89 keV in ^{186}Tl. Relatively strong 6472 keV-281 keV coincidences point to the existence of a low-energy 75 keV γ transition from the state at 356 keV to the state at 281 keV, see fig. 7. Unfortunately, apart from being possibly strongly converted, this transition is close in energy to the Tl K X-rays and no solid identification can be given for the 75 keV decay, which is, therefore, shown in fig. 7 in brackets as a tentative transition.

We mention that the weak 6390 keV and 6475 keV α lines have been seen in [7] in the spectra, collected at mass $A = 190$, but no assignment could be made.

The decay scheme of ^{190m1}Bi $\rightarrow^{186m1}$Tl, based on the previous and new data, is shown in fig. 7. The spin and parity assignments will be discussed in sect. 4.

3.2.2 The α-decay of the low-spin isomer

A few new fine-structure decays of the low-spin isomer in ^{190}Bi were identified in this experiment (see table 2).

The $Q_{\alpha,\mathrm{sum}} = 6864(10)$ keV for the 6412(10) keV-314(1) keV group of events (fig. 5a and fig. 6e) is consistent with the $Q_{\alpha,\mathrm{sum}} = 6863(5)$ keV for the strongest 6431 keV-294 keV decay of ^{190m2}Bi. On these grounds, the 6412 keV decay was assigned to a fine-structure decay of ^{190m2}Bi populating a new excited state at 314(1) keV in ^{186m2}Tl.

Fig. 6b shows the events in coincidence with the 6611(10) keV decay (events from box B of fig. 5a), in which, along with the strong Tl K X-rays, a peak at 105(1) keV is seen. The shape of box B is due to the α-e$^-$ summing effect (see below). The value $Q_{\alpha,\mathrm{sum}} = 6858(10)$ keV establishes the 6611 keV decay as a fine-structure decay of ^{190m2}Bi feeding a new excited state at 105(1) keV in ^{186m2}Tl. By comparing the numbers of the Tl K X-rays and 105 keV decays, a K-conversion coefficient of $\alpha_K = 36(5)$ was deduced, which determines an $M2$ multipolarity for this decay ($\alpha_K(M2,\mathrm{theor.}) = 41$, $\alpha_K(M1,\mathrm{theor.}) = 6.4$, $\alpha_K(E1,E2,\mathrm{theor.}) \leq 0.6$ [22]). The resulting α(6611 keV)-e$^-$ summing in the PSSD with the conversion electron energy of ≈ 20 keV (plus the Auger electron energy of ≈ 10 keV in case of K_α-conversion) produces the 6640(10) keV-K_α and 6630(10) keV-K_β coincident events, seen in fig. 5a, which explains the non-rectangular shape of the box B.

We mention that a weak 6617 keV α line was seen in [7] in the spectra, collected at mass $A = 190$, but could not be identified.

Figure 6d shows the events from box D of fig. 5a, in which, along with the Tl K X-rays, the γ peaks at 105(1), 111(1) and 79(1) keV are seen. The position of this box at $E_\alpha = 6450$–6500 keV is due to the α(6431 keV)-e$^-$ summing (see below). The observed 79 keV transition represents, most probably, the 78.5 keV decay seen in coincidence with the 6431 keV α-decay of ^{190m2}Bi in [7].

The energy sum of these three transitions equals 295 keV, which fits within the error bars to the energy of the known (3^+) state at 293.7 keV in ^{186}Tl. On this basis we tentatively place these transitions in a cascade, de-exciting the 294 keV state. This conclusion is supported by the observation of coincidences between the 79 keV decay and the Tl K X-rays for the events from box D of fig. 5a (see also fig. 6d). The Tl K X-rays originate presumably

from the strongly converted coincident decay at 105 keV and, possibly, at 111 keV (see below).

In [7] the 78.5 keV transition was placed to de-excite the 293.7 keV level directly as no other coincidences in a cascade were observed (except for the Tl K X-rays, see fig. 11 of [7]). Furthermore, a decay at 6507(5) keV (see table 2) was observed in the spectra, taken at mass $A = 190$. Based on the $Q_{\alpha,\mathrm{sum}}$ value analysis it was attributed as a fine-structure α-decay of $^{190\mathrm{m2}}$Bi feeding an excited state 78.5 keV below the state at 293.7 keV. In our case, due to a large background in the corresponding part of the spectra and α-e$^-$ summing effects, we could not identify this α-decay. Therefore, we assumed the presence of the 6507 keV decay from the data of [7] and also placed the 79 keV decay as directly de-exciting the state at 294 keV, see fig. 7. The non-observation in [7] of the γ-γ coincidences between the transitions from the 79-111-105 keV cascade is readily explained by the much lower number of counts along with a relatively large conversion coefficient of the 105 keV and 111 keV transitions. The latter statement is confirmed by the low, but comparable intensity for the 105 keV and 111 keV decays in fig. 5d. Based on the intensity balance and measured conversion coefficient of the 105 keV decay, this excludes an $E1$ multipolarity for the 111 keV decay ($\alpha_{\mathrm{tot}}(\mathrm{theor.}) = 0.33$), but an $M1$, $E2$ or $M2$ multipolarity cannot be excluded, as the total theoretical conversion coefficients are: 6.6($M1$), 3.9($E2$) and 51($M2$). However, due to a rather large background and complexity of the α-γ spectra in this work we prefer not to draw any conclusion on the multipolarity of the 111 keV transition.

Under an assumption of the cascade character of the 105 keV and 79 keV decays, a total conversion coefficient of $\alpha_{\mathrm{tot}} = 0.3(2)$ for the latter decay can be deduced by comparing the number of Tl K X-rays with the number of 79 keV decays in fig. 5d. This suggests an $E1$ multipolarity for the 79 keV decay, as the theoretical values are $\alpha_{\mathrm{tot}}(E1) = 0.14$, $\alpha_{\mathrm{tot}}(M1) = 3$, $\alpha_{\mathrm{tot}}(E2, M2) \geq 16$.

Due to the relatively high conversion coefficients of the 105 keV and 111 keV transitions and subsequent α(6431 keV)-e$^-$ summing in the PSSD, the energy of the 6431 keV decay in coincidence with these decays and with the K X-rays is shifted to higher values. The shift amounts to about 30 keV if only one of the 105 keV and 111 keV transitions is K-converted, about 60 keV if both transitions are K-converted (the most probable case) and about 120 keV if one of them is K-converted, while the second one is L-converted (for example, the ratio $K/L \approx 2.25$ for a 105 keV $M2$ transition). These shifts explain both the position of the box D and the appearance of multiple peaks in fig. 5a in the region of $E_\alpha = 6450$–6650 keV and $E_\gamma \leq 120$ keV.

One more group with about 30 counts at 6225(10) keV-213(1) keV was observed in the α-γ matrix. The value $Q_{\alpha,\mathrm{sum}} = 6572(10)$ keV for this group matches the $Q_\alpha = 6569(5)$ keV value for the strongest 6431 keV decay of $^{190\mathrm{m2}}$Bi and on this basis we assign the 6225 keV decay as a fine-structure decay of $^{190\mathrm{m2}}$Bi feeding a new excited state at 213(1) keV above the state at 294 keV (thus, at 507 keV) in $^{186\mathrm{m2}}$Tl, see fig. 7. No information on the multipolarity of the 213 keV decay could be deduced.

Figure 7 shows the deduced decay scheme of ^{190}Bi, while table 2 summarises the data from this work and from [7].

4 Discussion

4.1 Proton-neutron multiplets in odd-odd Tl and Bi isotopes close and beyond the neutron mid-shell at N = 104

Spectroscopic studies of the odd-odd Bi and Tl isotopes are difficult due to a variety of rather closely lying configurations expected in these nuclei. In the previous α-decay studies of the $^{190-196}$Bi nuclei [6,7] the unhindered $10^- \rightarrow 10^-$ and $3^+ \rightarrow 3^+$ α-decays between the normal states in the parent Bi isotopes and intruder states in the daughter Tl isotopes, respectively, have been investigated. Additionally, rather strongly hindered (HF $\approx 10^3$, relative to the $10^- \rightarrow 10^-$ and $3^+ \rightarrow 3^+$ decay) $10^- \rightarrow 7^+$ and $3^+ \rightarrow 2^-$ α-decays between the normal states in the parent and daughter nuclei were observed for the first time.

Table 3 summarises main configurations and I^π assignments expected in $^{188-196}$Bi and their daughters $^{184-192}$Tl (see [7] and references therein for the detailed discussion). In the vicinity of the neutron mid-shell at $N = 104$, the states observed at low excitation energy in these nuclei, in particular in ^{190}Bi and ^{186}Tl, result mainly from coupling of the odd proton, moving either in the $\pi 3s^{-1}_{1/2}$ or in the intruder $\pi 1h_{9/2}$ orbital, to the odd neutron in the $\nu 3p_{3/2}$ or $\nu 1i_{13/2}$ orbital. Thus, full p-n multiplets appear and the relative ordering of the states will mainly result from the specific proton-neutron residual interaction acting in these $(j_\mathrm{p} \otimes j_\mathrm{n})J$ configurations.

We do not consider a $\nu 2f_{5/2}$ configuration as it is expected to be at a much higher excitation energy in Tl and Bi isotopes close to the neutron mid-shell (see the discussion in [7] and fig. 4 of [8]).

Recently low-lying $13/2^+$ isomeric states were observed in ^{187}Bi (at 252 keV, [25]) and in ^{189}Bi (at 357 keV, [18,25]). They were interpreted as a proton excitation into the $\pi 1i_{13/2}$ valence orbital and their downsloping trend in excitation energy by approaching the mid-shell at $N = 104$ was mainly explained through the proton-neutron interaction with the valence neutrons in the $\nu 1i_{13/2}$ orbital. Furthermore, the experimental trend and the results of study [25] suggest that in the lighter odd-mass Bi nuclei the $13/2^+$ state may even become the ground state. That is why we included the corresponding configurations for the odd-odd mass Bi nuclei in table 3. In the daughter Tl nuclei the situation is different. Since the excited states based on the low-lying (oblate and prolate) $\pi 1i_{13/2}$ configurations in the odd-mass Tl isotopes close to the neutron mid-shell were found at higher energies (≈ 1 MeV and above, see [26] and references therein), we did not consider such configurations for the odd-odd Tl nuclei discussed in this work. This is in contrast to oblate

Table 3. Main configurations and I^π assignments expected in $^{188-196}$Bi and their daughters $^{184-192}$Tl. The last column shows the observed states in ^{188,190}Bi and in ^{184,186}Tl. Note that the I^π assignments in column 3 are tentative and based on systematics and α-decay data, such as HF values and decay characteristics, as discussed in the text.

Configuration	Possible I^π	Observed I^π
Bi, normal states ($\pi 1h_{9/2}$ or $\pi 1i_{13/2}$)		
$[\pi 1h_{9/2} \times \nu 3p_{3/2}]$	$3^+ \rightarrow 6^+$	3^+
$[\pi 1h_{9/2} \times \nu 1i_{13/2}]$	$2^- \rightarrow 11^-$	10^-
$[\pi 1i_{13/2} \times \nu 3p_{3/2}]$	$5^- \rightarrow 8^-$	
$[\pi 1i_{13/2} \times \nu 1i_{13/2}]$	$0^+ \rightarrow 13^+$	
Tl, normal states ($\pi 3s^{-1}_{1/2}$ or $\pi 2d^{-1}_{3/2}$)		
$[\pi 3s^{-1}_{1/2} \times \nu 3p_{3/2}]$	1^-,2^-	2^-
$[\pi 3s^{-1}_{1/2} \times \nu 1i_{13/2}]$	$6^+, 7^+$	$6^+, 7^+$
$[\pi 2d^{-1}_{3/2} \times \nu 3p_{3/2}]$	$0^- \rightarrow 3^-$	
$[\pi 2d^{-1}_{3/2} \times \nu 1i_{13/2}]$	$5^+ \rightarrow 8^+$	
Tl, intruder states (*based on* $\pi 1h_{9/2}$)		
$[\pi 1h_{9/2} \times \nu 3p_{3/2}]$	$3^+ \rightarrow 6^+$	3^+
$[\pi 1h_{9/2} \times \nu 1i_{13/2}]$	$2^- \rightarrow 11^-$	10^-

intruder $\pi 1h_{9/2}$ configuration which was typically found at a lower excitation energy [26].

A configuration which involves a $\pi 2d^{-1}_{3/2}$ proton hole is also shown in table 3 for the Tl isotopes. The low-lying single-particle $3/2^+$ proton hole states are known in the odd-mass $^{183-201}$Tl at a nearly constant excitation energy of only about 250–400 keV above the $1/2^-$ ($\pi 3s^{-1}_{1/2}$) ground state (see fig. 3.13 of [1] and ref. [27]). Therefore, one would expect the low-lying excited states at similar energies in the odd-odd Tl nuclei, resulting from the coupling of a valence neutron to such states in the odd-mass Tl isotopes.

Finally, for the lightest Bi and Tl isotopes beyond the neutron mid-shell at $N = 104$ the neutron $1i_{13/2}$ state will start moving up in energy, while the neutron hole excitations into the $2f_{7/2}$ or $1h_{9/2}$ orbitals may start playing a role in the low-energy part of the spectrum (not shown in table 3).

As a first approximation, Paar's rule [28] which results in an energy splitting within a given proton-neutron multiplet that depends quadratically on spin $J(J+1)$ can be applied in many cases to deduce relative positions of the multiplet states. Furthermore, more advanced calculations within the framework of the two-quasiparticle plus rotor model and the proton-particle neutron-quasiparticle quadrupole vibrator model were used by different authors with the aim of shedding light on possible configurations and multiplet energy splittings in the odd-odd Tl and Bi nuclei (see references and review in [8]). In particular, an explicit proton-neutron interaction, approximated by a zero-range force including spin exchange is taken into account in [8] besides the coupling of the proton and neutron orbitals to low-lying quadrupole vibrations of the underlying core. It can be also shown that the particle-core coupling approach used in [8] precisely gives rise to a quadratic expression in $J(J+1)$, using second-order perturbation theory when evaluating the energy splitting of the p-n multiplet members (see appendix of ref. [8]). In this respect the Paar's rule can be considered as a particular case of a more general approach of ref. [8].

As a specific example, relevant to the present study, we recall the results of the calculations [8] for the $[\pi 1h_{9/2} \times \nu 1i_{13/2}]_{2^- \rightarrow 11^-}$ configuration in the odd-odd Tl and Bi isotopes.

First of all, we underline that the calculated energy splitting and relative position of the states within a given multiplet depend on the neutron occupation probabilities u^2 and v^2 as a function of the neutron number, see [8]. In particular, around a value of $v^2(1i_{13/2}) \approx 0.5$–$0.6$ ($N \approx 107$–109 in Tl nuclei, see fig. 8 and table 4 of [8]), the p-n coupling and hence the multiplet splitting will be changing from particle-hole–like (for the heavier nuclei) to particle-particle–like (for the lower-mass nuclei). Therefore, depending mostly on the neutron single-particle energies and the pairing force parameters an uncertainty of about 2 mass units for the mass-dependence of the calculated results should be considered.

As shown in fig. 8 of [8] in the odd-odd Tl isotopes with $A(\mathrm{Tl}) > 188$ the 8^- state is expected to be the *lowest* member of this multiplet, which is indeed the case in $^{192-198}$Tl [5–7]. In some cases (for example in ^{188,190}Tl) other high-spin members of this multiplet (*e.g.*, 9^-, 10^-) were observed via α-decay studies of the high-spin 10^- isomer in the parent Bi isotopes [6,7]. In contrast, mainly due to a relatively high excitation energy (and a large angular-momentum difference between parent and daughter states in case of the high-spin isomer in Bi nuclei) the low-spin members of this multiplet could not generally be observed in the α-decay studies. The situation changes for $A(\mathrm{Tl}) < 188$ nuclei, in which the 8^- state is predicted to become the *highest* state of the multiplet. The 10^- state is expected to stay below the 8^-, 9^- and 11^- states, thus possibly becoming an isomeric state with a relatively long half-life. These predictions are in agreement with experimental data for ^{186}Tl ([7] and fig. 7 of this paper) and with our new data for ^{184}Tl (see fig. 4 and the discussion

below). They are also in agreement with the calculations, performed within Paar's approach [28]. An important result of these calculations, relevant for this work, is that for $A(\mathrm{Tl}) < 188$, the 6^- and 7^- multiplet states are predicted to stay slightly above the 10^- state, while the low spin 2^-–5^- states are expected to stay below the 10^- state. Therefore, some of these low-spin relatively low-lying 2^-–5^- states can be populated via α-decay of the low-spin isomer in the parent Bi nuclei, which was difficult in the heavier nuclei.

In the parent odd-odd Bi nuclei the situation is somewhat more complicated. The 10^- state of the $[\pi 1h_{9/2} \times \nu 1i_{13/2}]$ multiplet was predicted (fig. 9 of [8]) to be the lowest (isomeric) multiplet member in the heavier isotopes, which was experimentally confirmed down to ^{190}Bi ($N = 107$) in ref. [7]. Below the neutron number $N = 107$ the 8^- state is expected [8] to become slightly lower than the 10^- state (though by a few tens of keV only), which would mean that the 10^- state will not be an isomeric state any more. Combined with a predicted level sequence change of the $[\pi 1h_{9/2} \times \nu 1i_{13/2}]_{2^-\rightarrow 11^-}$ multiplet in the daughter Tl nuclei with $A < 188$, the decay pattern of the $A(\mathrm{Bi}) < 190$ isotopes (especially of a low-spin isomer) may change significantly. However, the results of calculations were rather sensitive to the choice of parameters and therefore should be considered as indicative only. For example, as shown below, our new data for ^{188}Bi prove that the 10^- state is still the lowest state of the $[\pi 1h_{9/2} \times \nu 1i_{13/2}]$ multiplet in this nucleus.

We mention also that a coupling between the various multiplets may be quite important in some cases. With this information in mind we proceed to discuss our new results on ^{188,190}Bi, while ^{184,186}Bi and their daughter isotopes will be discussed in [20].

4.2 α-decay of ^{190}Bi

Our data confirm the main conclusions of the work [7] on known α-decays of $^{190\mathrm{m1,m2}}$Bi (see table 2 and discussion in sect. 3). Therefore, in this section we will concentrate on the new data for the fine-structure α-decays.

4.2.1 High-spin isomer $^{190\mathrm{m1}}$Bi and excited states in the daughter $^{186\mathrm{m1}}$Tl

A few experimental facts should be considered for establishing the possible spin and parity assignments of the new excited states at 441, 356, 281 and 255 keV in $^{186\mathrm{m1}}$Tl. First of all, the long-lived $T_{1/2} = 2.9$ s (10^-) state at 374 keV in $^{186\mathrm{m1}}$Tl was interpreted as a $[\pi 1h_{9/2} \times \nu 1i_{13/2}]_{10^-}$ multiplet member ([7,8] and sect. 4.1). Hence, the non-observation of decays from this state to the states at 356, 281 and 255 keV establishes un upper limit for their spin/parity as $7^{+,-}$. The 8^+ assignment for any of these three states is excluded as the resulting $M2$ decay, although possibly hindered, would still be much faster than the measured half-life of the 374 keV state. On the other hand, the observation of fast ($\Delta T(\alpha\text{-}\gamma) < 5$ μs) transitions from these three states to the known (6^+) and/or (7^+) states in $^{186\mathrm{m1}}$Tl limits corresponding transition multipolarities to $\Delta L \leq 2$. Altogether, this results in a range of $I = 5$–7 for the spin values of the states at 356, 281 and 255 keV. Based on the same arguments the possible spin range for the 441 keV state is $I = 5$–8.

As one can see from table 3 in the odd-odd Tl nuclei, only two configurations are capable of producing (previously unobserved) states with a spin in the required range of 5–7 (or 5–8, in case of the 441 keV state): $[\pi 2d_{3/2}^{-1} \times \nu 1i_{13/2}]_{5^+\rightarrow 8^+}$ and $[\pi 1h_{9/2} \times \nu 1i_{13/2}]_{2^-\rightarrow 11^-}$. Therefore below we will discuss possible assignments, based on these two configurations.

Considering the $[\pi 2d_{3/2}^{-1} \times \nu 1i_{13/2}]$ configuration we note that the excitation energies of the $\pi 2d_{3/2}^{-1}$ hole states in the neighbouring odd-mass ^{185}Tl and ^{187}Tl isotopes are 284 keV and 300 keV, respectively (fig. 3.13 of [1]) and therefore one expects the states resulting from this particular proton-neutron multiplet to be at similar excitation energies. On these grounds, one could tentatively assign the states at 441, 356, 281 and 255 keV as the members of the $[\pi 2d_{3/2}^{-1} \times \nu 1i_{13/2}]_{5^+\rightarrow 8^+}$ multiplet. As explained above, the 8^+ member of this multiplet cannot be below the long-lived isomeric (10^-) state at 374 keV and therefore the 441 keV state could be tentatively assigned the spin and parity of $I^\pi = (8^+)$. In such a case, the states at 356, 281 and 255 keV should have the spin and parity of $5^+ \rightarrow 7^+$. This scenario is in general agreement with the predictions of the Paar's rule [28]. Namely, for the coupling of a hole in the $\pi 2d_{3/2}$ orbital and a quasiparticle in the $\nu 1i_{13/2}$ orbital a very specific ordering of the $5^+ \rightarrow 8^+$ states can be deduced with the 5^+ and 8^+ states as the higher-lying ones and the 6^+ and 7^+ states as the lower-lying closely spaced ones. Taking into account all above arguments, the state at 356 keV should have $I^\pi = (5^+)$, while the states at 281 and 255 keV should be assigned the values of (6^+) and (7^+) or vice versa, as the relative spacing within the multiplet is somewhat sensitive to the choice of parameters in the calculations, see [28].

If these states belong to the same multiplet, prompt $M1$ intra-multiplet transitions should be expected and evidence for one such transition (at 75 keV) was tentatively suggested in our work (see fig. 7 and discussion in sect. 3.2.1). The apparent non-observation of the other intra-multiplet decays can be readily explained, first of all, by a rather strong internal conversion of such low-energy $M1$ transitions ($\alpha_{\mathrm{tot}}(\mathrm{theor.}) \approx 10$ for the 50–100 keV $M1$ decays), by the complexity of the spectra and by the low intensity. Furthermore, the competition from direct higher-energy decays to the lowest 6^+ and/or 7^+ states in $^{186\mathrm{m1}}$Tl is another reason for the non-observation of intra-multiplet transitions.

Still assuming that the 441, 356, 281 and 255 keV states belong to the $[\pi 2d_{3/2}^{-1} \times \nu 1i_{13/2}]$ multiplet we point out that the α-decays at 6392 and 6472 keV feeding the 441 and 356 keV states, respectively, have quite similar HF values (235(40) and 275(50), respectively), see fig. 7. These values are strongly different from the HF of 4700(800) and

6600(1200) for the 6546 keV and 6570 keV decay, feeding the 281 and 255 keV states, respectively. Tentatively this could be related to the fact that in the case of the (5^+) and (8^+) states the angular momenta of the valence proton and neutron are fully aligned and coupled either anti-parallel (5^+ state) or parallel (8^+ state) to each other, the latter being similar to the case of the nearly parallel alignment in the (10^-) state of the parent ^{190m1}Bi. This is different for the (6^+) and (7^+) multiplet states in Tl nuclei as these states require an intermediate angular-momentum coupling.

Alternatively, to explain the large hindrance factor difference one could assume that the states at 441 and 356 keV result from a different configuration, compared to the states at 281 and 256 keV. In this case the state at 441 keV could potentially be one of the $(6,7,8,9,11)^-$ members of the $[\pi 1h_{9/2}\times\nu 1i_{13/2}]$ multiplet, which are predicted to stay slightly above the 10^- state in ^{186}Tl (see sect. 4.1). Most probably, in any of these cases the direct 352 keV and 441 keV transitions to the lowest (6^+) and (7^+) states in ^{186m1}Tl, respectively, would dominate over the low-energy (≤ 67 keV) strongly converted intra-band transition(s) to the long-lived (10^-) state at 374 keV in ^{186m1}Tl. The state at 356 keV can potentially be a 5^- state of the $[\pi 1h_{9/2}\times\nu 1i_{13/2}]$ multiplet, which is predicted to stay below the 10^- state in ^{186}Tl. The states at 281 keV and 256 keV, populated by the more strongly hindered α-decays could still be the (6^+) and (7^+) states (or vice versa) of the $[\pi 2d^{-1}_{3/2}\times\nu 1i_{13/2}]$ configuration. In such a case the lower hindrance factors for the 6392 and 6472 keV α-decays to the states at 441 and 356 keV could be explained by the same $[\pi 1h_{9/2}\times\nu 1i_{13/2}]$ configuration in the parent and daughter nuclei. The observed difference in the hindrance factors for the 6392, 6546 and 6472 keV α-decays in this case would probably arise from the different proton-neutron angular-momentum coupling in the daughter states.

The assumption of the $[\pi 2d^{-1}_{3/2}\times\nu 1i_{13/2}]$ configuration for the states at 281 and 255 keV requires a change of a $1h_{9/2}$ proton particle in the parent Bi nucleus to a $2d_{3/2}$ proton hole in the daughter Tl isotope. Most probably, this would lead to an additional hindrance compared to the α-decays to the lowest (6^+) and (7^+) states of the $[\pi 3s^{-1}_{1/2}\times\nu 1i_{13/2}]$ configuration and based on our data this additional hindrance can be estimated as 4–6 (see fig. 7).

To conclude this part, based on the available experimental data alone, only a spin range of $I = 5$–8 can be given for the 441 keV state and a spin range of $I = 5$–7 for the states at 356, 281 and 255 keV in ^{186m1}Tl. The most probable configurations, responsible for these states, are $[\pi 1h_{9/2}\times\nu 1i_{13/2}]$ and $[\pi 2d^{-1}_{3/2}\times\nu 1i_{13/2}]$, but no definitive assignments can be established.

4.2.2 Low-spin isomer ^{190m2}Bi and excited states in the daughter ^{186m2}Tl

New excited states have been also observed in the decay of the low-spin isomer in ^{190}Bi, see fig. 7. Possibly, some of these states may belong to the $[\pi 2d^{-1}_{3/2}\times\nu 3p_{3/2}]_{0^-\rightarrow 3^-}$ multiplet (see table 3 and cf. the discussion of the $[\pi 2d^{-1}_{3/2}\times\nu 1i_{13/2}]$ multiplet above). Furthermore, the low-spin $2^-\rightarrow 5^-$ states of the intruder $[\pi 1h_{9/2}\times\nu 1i_{13/2}]$ multiplet in ^{186}Tl cannot be excluded as they are predicted to stay below the 10^- state of this multiplet (see sect. 4.1). In this case α-decays from the $[\pi 1h_{9/2}\times\nu 3p_{3/2}]_{3^+}$ state in ^{190m2}Bi to both of these configurations will be somewhat hindered, as they would require a $\pi 1h_{9/2}\rightarrow\pi 2d^{-1}_{3/2}$ change in the former case, or a $\nu 3p_{3/2}\rightarrow\nu 1i_{13/2}$ in the latter case.

Unfortunately, due to the lack of definitive data on the multipolarity of some of the transitions and a rather complex decay pattern we prefer not to draw any conclusions on the possible spin and parity of these states.

The reduced α widths δ^2_α calculated with the Rasmussen prescription [9] for unhindered $\Delta L = 0$ α-decays of ^{190}Bi are: δ^2_α(6456 keV, ^{190m1}Bi) = 33(6) keV and δ^2_α(6431 keV, ^{190m2}Bi) = 55^{+20}_{-7} keV. These values show that similar to the heavier ^{192,194,196}Bi nuclei, the $3^+\rightarrow 3^+$ α-decay in ^{190}Bi is somewhat more favoured than the $10^-\rightarrow 10^-$ decay (see also table 1 of [7]).

The following sections will provide more information on the systematics of the fine-structure α-decays in $^{188-196}$Bi and on the excited states in the daughter Tl isotopes.

4.3 α-decay of ^{188}Bi

4.3.1 The α-decay of the high-spin isomer ^{188m1}Bi and the new intruder (10^-) state at 500 keV in ^{184m1}Tl.

The energies of the known 6813 keV and the new 7302 keV α-decays of ^{188m1}Bi fit well to the systematics of the $10^-\rightarrow 10^-$ and $10^-\rightarrow 7^+$ decays, respectively, in the heavier odd-odd Bi isotopes, see fig. 8a. On these grounds, we tentatively assign the spin and parity of (10^-) to the isomeric state with $T_{1/2} = 265(15)$ ms in ^{188}Bi and the spin and parity of (7^+) to the state in the daughter ^{184}Tl, fed by the 7302 keV decay. Based on the unhindered nature of the 6813 keV decay we interpret the new excited state at 500 keV in ^{184m1}Tl as a (10^-) member of the intruder $[\pi 1h_{9/2}\times\nu 1i_{13/2}]_{2^-\rightarrow 11^-}$ multiplet. As discussed in sect. 4.1, this state is expected to stay below the 8^-, 9^- and 11^- multiplet states in ^{184}Tl, thus possibly becoming an isomeric state (as in ^{186}Tl, see fig. 7). The non-observation of the direct 500 keV γ-decay to the lowest (7^+) state in ^{184m1}Tl is in agreement with the above assignment as such a transition would be of an $E3$ multipolarity with a much longer half-life than the interval of 5 μs for the α-γ coincidences in our experiment. This state extends the systematics of the 10^- intruder states in the odd-odd mass Tl nuclei, see fig. 8b. The energy systematics can be approximated by a parabolic dependence on the number of valence pairs outside the neutron closed-shell configuration, counted as holes from the $N = 126$ shell and as particles from the $N = 82$ shell (see refs. [2,3]

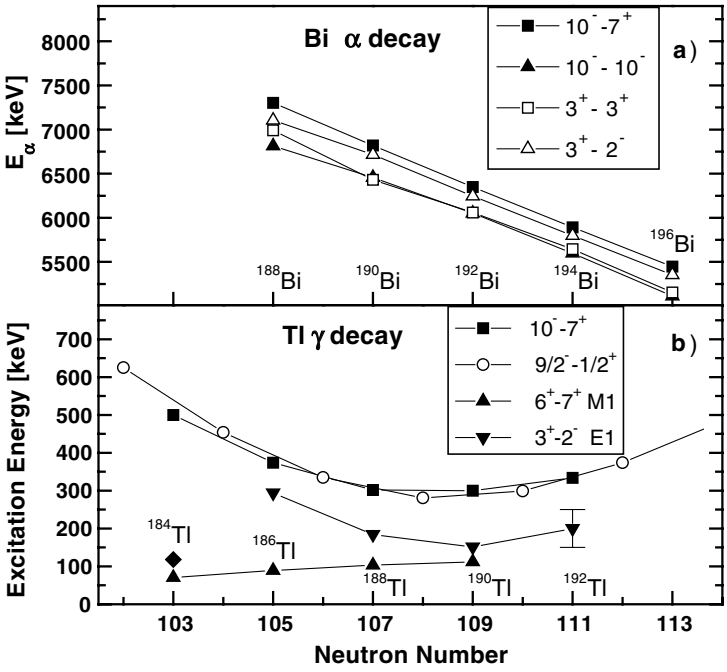

Fig. 8. a) Systematics of some selected α-decays in the odd-odd $^{188-196}$Bi isotopes; b) systematics of the excitation energies of some selected γ transitions in the daughter odd-odd $^{184-192}$Tl isotopes and of the $9/2^-$ intruder states in the odd-mass $^{183-193}$Tl. The excitation energies are given relative to the lowest state in *each particular isomer*. The $10^- \rightarrow 7^+$ and $3^+ \rightarrow 2^-$ α-decay energies are not known in ^{196}Bi, but can be deduced from fig. 2 of ref. [7]. The position of the excited state at 117.5 keV in ^{184}Tl is shown by a full diamond. Data are from this work and from refs. [7,29].

for more details). Therefore, in the remainder of this discussion, we shall speak about the "parabolic energy dependence" when referring to this phenomenon of intruder energy variation.

The (7^+) assignment for the lowest state in ^{184m1}Tl and an $M1$ multipolarity for the 70.5 keV transition establish the spin and parity of (6^+) for the excited state fed by the 7232 keV decay of ^{188m1}Bi. Similar to $^{186-190}$Tl [7], this state is most likely the second member of the $[\pi 3s_{1/2}^{-1} \times \nu 1i_{13/2}]_{6^+,7^+}$ doublet. This extends the systematics of such states up to ^{184}Tl and confirms the downward trend of their excitation energy relative to the lowest (7^+) state: 112.2 keV in ^{190}Tl, 103.1 keV in ^{188}Tl, 89.5 keV in ^{186}Tl and 70.5 keV in ^{184}Tl (see fig. 8b).

By analogy with the decay of the high-spin isomer in ^{190}Bi, the state at 320 keV in ^{184m1}Tl can be attributed as one of the $I = (5\text{–}7)$ members of the $[\pi 2d_{3/2}^{-1} \times \nu 1i_{13/2}]_{5^+ \rightarrow 8^+}$ multiplet or, possibly, as a $[\pi 1h_{9/2} \times \nu 1i_{13/2}]_{5^-}$ state. Indeed, the non-observation of the decay from the long-lived state at 500 keV establishes an upper limit on the spin and parity of the 320 keV state as $7^{-/+}$. On the other hand, the observation of the fast decays from the 320 keV state to the (7^+) and (6^+) states in ^{184m1}Tl requires its spin to be not lower than 5. Other members of these multiplets could not be observed in this experiment presumably due to a lower number of events compared to ^{190m1}Bi.

It is important to underline the practically linear dependence of the energy of the $(10^-) \rightarrow (7^+)$ α-decays on the Bi mass number (see fig. 8a). Indeed, a linear fit (not shown in the figure) of the data for $^{188-194}$Bi reproduces the measured values with an error in each point close to the uncertainty of the α energy measurements. In contrast, the energy of the $(10^-) \rightarrow (10^-)$ decays follows a parabolic dependence as a function of the number of valence nucleon pairs with a local maximum in ^{192,194}Bi (not seen clearly due to the scale chosen for the Y-axis in fig. 8a). The latter trend reflects the well-known parabolic behaviour of the energy of the intruder 10^- states as a function of the neutron number in the daughter Tl isotopes (see fig. 8b) and the new state at 500(5) keV in ^{184m1}Tl fits well to these systematics. Furthermore, fig. 8b clearly illustrates the similar behaviour of the 10^- and $9/2^-$ intruder states in the odd-odd and odd-mass Tl isotopes, respectively. The so-called "scaling law", which is responsible for such a behaviour, was discussed in [3,6,7] and we refer the reader to these papers. The fact that both $10^- \rightarrow 7^+$ and $10^- \rightarrow 10^-$ decays follow the systematics suggests the robustness of the underlying configurations, at least, up to ^{188m1}Bi and its daughter ^{184m1}Tl.

4.3.2 The α-decay of the low-spin isomer in ^{188}Bi

Figure 8a also shows the systematics of the known $3^+ \rightarrow 2^-$ and $3^+ \rightarrow 3^+$ α-decays of the low-spin isomers in the odd-odd $^{190-196}$Bi isotopes. Up to ^{190}Bi the $3^+ \rightarrow 2^-$ and $3^+ \rightarrow 3^+$ decays behave very similarly to the $10^- \rightarrow 7^+$ and $10^- \rightarrow 10^-$ decays discussed above: they follow the linear and the parabolic energy dependence, respectively,

on the neutron number. Moreover, the energies of the unhindered $10^- \rightarrow 10^-$ and $3^+ \rightarrow 3^+$ decays in $^{190-196}$Bi are very similar, the largest difference being only 46 keV (^{194}Bi, [7]).

Qualitatively, the known 6992 keV decay in ^{188m2}Bi follows the pattern observed for the $3^+ \rightarrow 3^+$ α-decays in the heavier Bi nuclei: it is an unhindered strongest decay, registered in coincidences with an $E1$ transition. According to the Paar's rule [28] the 3^+ state is expected to stay lowest in the $[\pi 1h_{9/2} \times \nu 3p_{3/2}]_{3^+ \rightarrow 6^+}$ multiplet for the A(Bi) < 198 nuclei, which was experimentally proved down to ^{190}Bi in [7]. Therefore, by analogy with the heavier odd-odd Bi nuclei, we tentatively assign the spin and parity of $I^\pi = (3^+)$ and the normal $\pi 1h_{9/2} \times \nu 3p_{3/2}$ configuration to the 60(3) ms isomer in ^{188}Bi.

The unhindered nature of the 6992 keV α-decay points to the same spin and parity of (3^+) for the state at 117.5 keV in the daughter ^{184m2}Tl, which is then interpreted as having an intruder $\pi 1h_{9/2} \times \nu 3p_{3/2}$ configuration. A hindered HF = 120(11) 7106 keV crossover transition feeds to a state with a possible assignment of $I^\pi = (2\text{–}4)^-$ which is defined by the deduced $E1$ multipolarity of the 117.5 keV decay. By analogy with the heavier odd-odd Tl isotopes we tentatively assign $I^\pi = (2^-)$ and $\pi 3s^{-1}_{1/2} \times \nu 3p_{3/2}$ configuration to this state.

However, in ^{188m2}Bi there are certain quantitative deviations from the decay pattern of the heavier odd-odd Bi isotopes. For example, the energy systematics in fig. 8a show that the assumed $(3^+) \rightarrow (3^+)$ 6992 keV decay has an energy about 200 keV higher than expected from the systematics. A deviation of about 100 keV to lower energies was also deduced for the assumed $(3^+) \rightarrow (2^-)$ 7106 keV decay. Furthermore, while the energy of the $E1$ transitions in coincidence with the unhindered α-decay of the low-spin isomers in $^{190-194}$Bi follows the parabolic energy dependence with a minimum in ^{190}Tl (151 keV, see fig. 8b), in ^{184}Tl it drops to 117.5 keV.

Finally, it is well known that in the complete-fusion reactions the high-spin isomer is usually more strongly populated than the low-spin isomer. This is indeed confirmed for $^{190-196}$Bi in which the intensity of the $10^- \rightarrow 10^-$ α-decay is higher (after normalisation on the corresponding b_α values) than the intensity of the $3^+ \rightarrow 3^+$ decay (see table 1 of [7] and fig. 1b of this paper for ^{190}Bi). However, in ^{188}Bi the situation is reversed: the 6813 keV $(10^-) \rightarrow (10^-)$ decay has lower intensity than the 6992 keV $(3^+) \rightarrow (3^+)$ decay, see fig. 1b (in both cases we assume $b_\alpha = 100\%$ taken from systematics). We also note that the reduced α widths $\delta^2_\alpha(6813 \text{ keV}, (10^-)) = 52(3)$ keV and $\delta^2_\alpha(6992 \text{ keV}, (3^+)) = 54(3)$ keV for strongest unhindered α-decays of ^{188}Bi are equal within the experimental uncertainty (assuming $\Delta L = 0$ decays). This is in contrast with the reduced α width systematics for the heavier $^{190-196}$Bi nuclei, in which the $3^+ \rightarrow 3^+$ α-decays were always more favoured (by (30–60)%) compared to the $10^- \rightarrow 10^-$ decays (see discussion for ^{190}Bi in sect. 4.1.2 and table 1 of [7]).

Unfortunately, based on the available data alone no explanation can be presently suggested for the observed deviations. Such a behaviour might indicate a change in the configuration of ^{188m2}Bi or in its daughter ^{184m2}Tl, or in both nuclei. As was mentioned in sect. 4.1, in the odd-odd Tl nuclei lighter than $A = 188$ the low-spin $I^\pi = 2^-$–5^- members of the $[\pi 1h_{9/2} \times \nu 1i_{13/2}]_{2^- \rightarrow 11^-}$ multiplet are expected at a relatively low excitation energy (at least, below the 10^- multiplet state). In such a way some of them can be populated via α-decay of the low-spin isomer in ^{188}Bi. Therefore, the presence of the new decay paths in the lighter Tl isotopes (compared to the A(Tl) > 188) may be one of the reasons for a change of systematics in the lighter Bi and Tl nuclei.

Another scenario for a possible change in the lighter odd-odd Bi nuclei is provided by the neighbouring odd-mass isotopes ^{187,189}Bi. In these isotopes the excitation energy of (presumably, oblate) intruder $1/2^+$ states does not follow a parabolic energy dependence on the neutron number, observed for the heavier odd-mass Bi isotopes (see the discussion in [27]). Moreover, the excitation energy of these states are quite low, being 112(11) keV in ^{187}Bi [27] and 230(30) keV [30] or 190(40) keV in ^{189}Bi [31]. The observed change of systematics may reflect the influence of expected oblate-prolate shape coexistence at low energy in the lightest odd-mass Bi nuclei and recently evidence for low-lying prolate rotational bands in ^{187,189}Bi was obtained [32]. Therefore, a possibility of an oblate-prolate shape coexistence at low excitation energy in the lightest odd-odd Bi isotopes should be also considered.

5 Conclusions

In this work we presented a detailed α-decay study of the neutron-deficient isotopes ^{188,190}Bi. A few new fine-structure lines in the α-decay of these nuclei were found, populating previously unknown excited states in the daughter ^{184,186}Tl isotopes. The most probable configuration of these states involves the coupling of the $1i_{13/2}$ neutron particle to the low-lying proton $2d^{-1}_{3/2}$ or $1h_{9/2}$ states in the neighbouring odd-mass Tl isotopes.

An intruder, presumably, $[\pi 1h_{9/2} \times \nu 1i_{13/2}]_{10^-}$ isomeric state at 500(5) keV was found in ^{184m1}Tl, extending the parabolic energy systematics of such states beyond the neutron mid-shell at $N = 104$.

The systematics of the $(10^-) \rightarrow (7^+)$ and $(10^-) \rightarrow (10^-)$ α-decays of the high-spin isomers in $^{188-196}$Bi suggest the robustness of the underlying configurations, at least, up to ^{188m1}Bi and its daughter ^{184m1}Tl. In contrast, the systematics of the assumed $(3^+) \rightarrow (2^-)$ and $(3^+) \rightarrow (3^+)$ α-decays of the low-spin isomers in $^{188-196}$Bi shows clear deviations in ^{188m2}Bi which may reflect the influence of the new configurations reported in the neighbouring odd-mass Bi nuclei.

More detailed complementary decay and in-beam γ spectroscopic studies, combined with spin measurements by means of laser spectroscopy, are necessary to understand such a behaviour.

The effect of the α-e$^-$ summing in the PSSD which is important for experiments at the recoil separators is discussed in detail and a few examples are presented.

We thank the UNILAC staff for providing the stable and high-intensity ^{50,52}Cr beams. This work was supported by the Academy of Finland, by the Access to Large Scale Facility programme under the Training and Mobility of Researchers programme of the European Union within the contract HPRI-CT-1999-00001, by the EXOTAG contract HPRI-1999-CT-50017, by the FWO-Vlaanderen and by the Interuniversity Attraction Poles Programme - Belgian State - Federal Office for Scientific, Technical and Cultural Affairs (IAP grant P5/07). K.V.d.V. is research assistant of the FWO-Vlaanderen. A.N.A. was partially supported by the GREAT contract EPSRC GR/M79981.

References

1. K. Heyde *et al.*, Phys. Rep. **102**, 291 (1983).
2. K. Heyde *et al.*, Nucl. Phys. A **466**, 189 (1987).
3. K. Heyde *et al.*, Nucl. Phys. A **484**, 275 (1988).
4. J.L. Wood *et al.*, Phys. Rep. **215**, 101 (1992).
5. A.J. Kreiner *et al.*, Phys. Rev. Lett. **47**, 1709 (1981).
6. M. Huyse *et al.*, Phys. Lett. B **201**, 293 (1988).
7. P. Van Duppen *et al.*, Nucl. Phys. A **529**, 268 (1991).
8. J. Van Maldeghem, K. Heyde, Fizika **22**, 233 (1990).
9. J.O. Rasmussen, Phys. Rev. **113**, 1593 (1959).
10. U.J. Schrewe *et al.*, Phys. Lett. B **91**, 46 (1980).
11. J. Schneider, GSI report GSI-84-3, 1984, unpublished.
12. J. Wauters *et al.*, Phys. Rev. C **55**, 1192 (1997).
13. P. Van Duppen, M. Huyse, Hyperfine Interact. **132**, 141 (2001).
14. G. Münzenberg *et al.*, Nucl. Instrum. Methods **161**, 65 (1979).
15. S. Hofmann *et al.*, Z. Phys. A **291**, 53 (1979).
16. S. Hofmann, G. Münzenberg, Rev. Mod. Phys. **72**, 733 (2000).
17. A.N. Andreyev *et al.*, Eur. Phys. J. A **6**, 381 (1999).
18. A.N. Andreyev *et al.*, Eur. Phys. J. A **10**, 129 (2001).
19. A.N. Andreyev *et al.*, Nature **405**, 430 (2000).
20. A.N. Andreyev *et al.*, this issue, p. 55.
21. J. Wauters *et al.*, Phys. Rev. C **47**, 1447 (1993).
22. The program to calculate conversion coefficients. The National Nuclear Data Center (NNDC), `http://www.nndc.bnl.gov/nndc/physco/`.
23. A.N. Andreyev, `http://npg.dl.ac.uk/GREAT/geant_gr.htm`; and Geant Detector Simulation Tool, CERN, 1993, `http://wwwinfo.cern.ch/asd/geant`.
24. F.P. Hessberger *et al.*, Nucl. Instrum. Methods A **274**, 522 (1989).
25. A. Hürstel *et al.*, Eur. Phys. J. A **15**, 329 (2002).
26. M. Muikku *et al.*, Phys. Rev. C **64**, 044308 (2001).
27. J.C. Batchelder *et al.*, Eur. Phys. J. A **5**, 49 (1999).
28. V. Paar, Nucl. Phys. A **331**, 16 (1979).
29. R.B. Firestone, *Table of Isotopes*, 8th edition (John Wiley and Sons, Inc., New York, 1996).
30. A.N. Andreyev *et al.*, Nucl. Instrum. Methods Phys. Res. A **330**, 125 (1993).
31. J.C. Batchelder *et al.*, Phys. Rev. C **52**, 1807 (1995).
32. A. Hürstel *et al.*, private communication (2002).